Acta Materialia 106 (2016) 78–86

Contents lists available at ScienceDirect

Acta Materialia

journal homepage: www.elsevier.com/locate/actamat

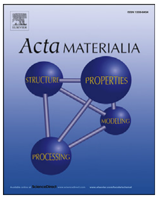

Full length article

# Expanding time–temperature-transformation (TTT) diagrams to interfaces: A new approach for grain boundary engineering

Patrick R. Cantwell [a], Shuailei Ma [b], Stephanie A. Bojarski [c], Gregory S. Rohrer [c], Martin P. Harmer [b], *

[a] *Department of Mechanical Engineering, Rose-Hulman Institute of Technology, 5500 Wabash Avenue, Terre Haute IN 47803, USA*
[b] *Department of Materials Science and Engineering, Center for Advanced Materials and Nanotechnology, Lehigh University, 5 East Packer Avenue, Bethlehem PA 18015, USA*
[c] *Department of Materials Science and Engineering, Carnegie Mellon University, 5000 Forbes Avenue, Pittsburgh PA 15213, USA*

## ARTICLE INFO

*Article history:*
Received 17 November 2015
Received in revised form
6 January 2016
Accepted 6 January 2016
Available online xxx

*Keywords:*
Grain boundaries (GBs)
Grain growth
Kinetics
Grain boundary engineering
Complexion

## ABSTRACT

Bulk phase transformation kinetics were not well understood before Davenport and Bain developed time–temperature-transformation (TTT) diagrams for steel alloys in the 1930s. These powerful diagrams revolutionized the heat treatment of steel and other alloys. Grain boundaries and internal interfaces are now known to behave in a phase-like manner, referred to as 'complexions', and their transitions can be represented on TTT diagrams. We present experimental grain boundary complexion TTT diagrams for polycrystalline $Al_2O_3$ and $Y_2O_3$. Grain boundary mobility discontinuities in $Y_2O_3$ occur at different temperatures for different annealing times, an unusual pattern that becomes understandable when viewed on a complexion TTT diagram. Similarly, the anisotropy of $Al_2O_3$ complexion kinetics can be visualized with these diagrams. Complexion TTT diagrams are a graphical tool to control interface-related phenomena such as diffusion, creep, oxidation, and microstructure evolution. They could explain why two-step sintering produces dense nanocrystalline ceramics and offer insight into other processes as well.

## 1. Introduction

Controlling the kinetics of bulk phase transformations is critical to controlling the microstructure and properties of a wide variety of solid state materials. The time it takes for an isothermal phase transformation to occur can be represented on a time–temperature-transformation (TTT) diagram, which in turn can be used to prescribe successful heat treatments for a variety of materials. The TTT diagram was developed by Davenport and Bain in 1930 [1] and was a breakthrough in understanding the kinetics of bulk phase transformations. The importance and utility of the TTT diagram was immediately recognized and played a pivotal role in advancing the state of the art of steel heat treatment in particular and materials processing in general.

Internal interfaces such as grain boundaries also play a crucial role in the processing and properties of materials. Grain boundary engineering was first proposed in 1984 by Watanabe [2] and since that time has become a highly active area of research. The overarching goal of grain boundary engineering is to control the grain boundary character distribution to produce materials with better performance and properties. More recently, it has been demonstrated unequivocally that grain boundaries and other internal interfaces behave in a phase-like manner [3], undergoing transitions that can change grain boundary properties such as mobility or diffusivity by orders of magnitude. These grain boundary complexion transitions have been traditionally referred to as grain boundary 'phase' transitions [4–6]. The term 'complexion' was proposed [7] to differentiate between interfaces (e.g. grain boundaries or phase boundaries) and bulk phases, and 'complexion' is the preferred nomenclature to describe phase-like transitions at grain boundaries [8].

As summarized in a recent review article [8], there is a substantial body of evidence demonstrating that grain boundaries behave in a phase-like manner and that different grain boundary complexions can have dramatically different properties. Complexion transitions have been described theoretically [9] and

---

* Corresponding author.
*E-mail addresses:* cantwep@rose-hulman.edu (P.R. Cantwell), mashuailei@gmail.com (S. Ma), sbojarski@gmail.com (S.A. Bojarski), rohrer@cmu.edu (G.S. Rohrer), mph2@lehigh.edu (M.P. Harmer).

http://dx.doi.org/10.1016/j.actamat.2016.01.010
1359-6454/

demonstrated via computer simulations and atomistic modeling [10–12]. When a grain boundary undergoes a complexion transition, its properties such as mobility, diffusivity, and cohesive strength may change discontinuously. In particular, mobility has been shown to change by over three orders of magnitude in alumina [13]. Presumably, all grain boundary-related properties will change somewhat during a complexion transition, but not necessarily by proportional amounts. For example, it is possible that the mobility can change by three orders of magnitude while the diffusivity only changes by an order of magnitude or less. This type of disparity could be exploited in grain boundary engineering. Several equilibrium complexion diagrams have been generated [8] but the importance of the kinetic transition behavior of complexions has been overlooked thus far. Based on their phase-like behavior, it stands to reason that grain boundary complexion transitions should be able to be represented on TTT diagrams in a manner analogous to bulk phase transitions. As such, grain boundary complexion TTT diagrams have the potential to impact the field of grain boundary engineering in the same way that bulk phase TTT diagrams impacted the heat treatment of steel alloys and other materials.

In this article, we present grain boundary complexion TTT diagrams for polycrystalline yttria ($Y_2O_3$) and alumina ($Al_2O_3$), two ceramic materials of technological interest and importance. Alumina and yttria are often doped with impurities to influence their microstructure development and enhance their properties. For example, Eu-doped $Y_2O_3$ sinters more readily and is more optically transparent than undoped $Y_2O_3$ [14], Yb/Er codoping of $Y_2O_3$ influences its optical emission behavior [15], and Y-doped $Al_2O_3$ has increased resistance to high-temperature creep due to yttrium segregation to grain boundaries [16]. Accordingly, the experiments used to develop the grain boundary complexion TTT diagrams presented here focus on two doped systems, Y-doped $Al_2O_3$ and Yb/Er codoped $Y_2O_3$.

Abnormal grain growth due to a discontinuous jump in grain boundary mobility is one of the most recognizable signs of a grain boundary complexion transition in doped ceramics [8]. Atomic-resolution transmission electron microscopy has shown that grain boundaries surrounding an abnormal grain have a chemistry and structure that is distinct from boundaries of normal grains [13]. Grain growth kinetics analysis has shown that the effective grain boundary mobility of these boundaries can be over three orders of magnitude higher than grain boundaries surrounding normal grains. Therefore, by monitoring grain growth as a function of time and temperature, it should be possible to map out the conditions under which grain boundary complexion transitions occur when subjected to isothermal annealing. The grain boundary complexion TTT diagrams presented in this work were generated by analyzing grain growth behavior in Y-doped $Al_2O_3$ and Yb/Er-doped $Y_2O_3$ under isothermal annealing conditions.

At the outset we point out that grain boundary complexion TTT diagrams are not identically analogous to bulk phase TTT diagrams because a grain boundary has five additional macroscopic degrees of freedom that describe its character. Three degrees of freedom describe the misorientation of the two grains on either side of the boundary and two degrees of freedom describe the grain boundary plane inclination. Therefore, each type of grain boundary will behave differently in thermodynamic terms and have its own TTT diagram. However, the microstructure development and properties of a polycrystalline material are often dominated by a subset of grain boundary complexions that all transition within a small temperature range and thus behave in a thermodynamically similar manner [8]. The result is that in many practical situations, grain boundaries of different character can be lumped together and treated as a group when plotting diagrams.

## 2. Experimental

Two types of $Y_2O_3$ powders were used in the present study. Yb/Er-doped $Y_2O_3$ experiments were carried out with a commercially produced powder co-doped with 10 wt.% $Yb_2O_3$ and 1 wt.% $Er_2O_3$ or 10 wt.% $Yb_2O_3$ and 4 wt.% $Er_2O_3$, with a starting particle size of about 200 nm (Orasure Technologies, Inc., Bethlehem, PA). For the undoped experiments, a high-purity $Y_2O_3$ powder (H. C. Starck GmbH & Co. KG, Goslar, Germany) was used, with a starting particle size less than 100 nm as determined by TEM analysis. The doped and undoped sintering specimens were produced directly from the as-received powders.

Impurities in the starting $Y_2O_3$ powders were quantified via inductively coupled plasma (ICP) analysis (Intertek Caleb Brett, Deer Park, TX) to determine the main impurities and their concentration. The impurities present in each powder are shown in Table 1. To avoid further contamination, the powder was uniaxially dry pressed in an alumina die under a low pressure (<1 MPa) to form disks of 14 mm diameter. The disks were then rubber-bagged and cold isostatically pressed at 35 MPa for 2 min. The green specimens were placed on a high purity alumina plate, covered with an alumina crucible, and fired in a box furnace at temperatures of 1000 °C–1600 °C in air. The heating and cooling rates were 6 and 5 °C/min, respectively. Soaking time at the sintering temperature varied from 0 to 24 h.

The bulk density of the $Y_2O_3$ sintered compacts was measured by the Archimedes immersion method using distilled water with 0.01% Brij-35 as a wetting agent. Samples for microstructural examination were cut from the core of the sintered pellet to avoid surface contamination effects, polished to a 1 μm finish, and thermally etched at a temperature 30 °C below the firing temperature for 15 min. Heating and cooling rates for the etching treatment were 10 °C/min.

The microstructure of the $Y_2O_3$ sintered samples was characterized by scanning electron microscopy (SEM) (Hitachi 4300; JEOL 6300F; Philips XL30 ESEM). The average grain size of each specimen was determined statistically by measuring about 1000 grains from the SEM images. Elemental analysis via energy dispersive X-ray spectroscopy (EDS) was done on a scanning transmission electron microscope (STEM) (VG Systems HB603) with a Nion Cs-corrector operating at 300 kV. X-ray diffraction (XRD) was conducted to identify the phases present in the powders and sintered specimens.

The Y-doped $Al_2O_3$ sandwich specimens were prepared as described elsewhere [17]. In brief, a bulk sample with (0001) and $(11\bar{2}0)$ single crystals of sapphire embedded in a 500 ppm Y-doped alumina polycrystal was spark plasma sintered, sectioned, and polished. Each sectioned sample was heated to a temperature between 1450 °C and 1600 °C for times between zero and fifteen

**Table 1**
Impurities concentrations determined by inductively coupled plasma mass spectrometry (ICP-MS) in the 10% Yb/1% Er-doped $Y_2O_3$ powder and the undoped $Y_2O_3$ powder, with units of wt. ppm (mg/kg). Doped $Y_2O_3$ contains more Al, Si, and Ca impurities than the undoped $Y_2O_3$.

| Element | 10%Yb/1%Er $Y_2O_3$ (ppm) | Undoped $Y_2O_3$ (ppm) |
|---|---|---|
| Al | 123 | < 10 |
| Si | 118 | < 10 |
| Ca | 62.9 | < 50 |
| Fe | 59.5 | < 10 |
| Na | 31.8 | 65.2 |
| K | 29.3 | 92.6 |
| Mg | 15.0 | < 10 |
| Zn | 9.6 | 14.6 |
| Cr | 5.6 | < 10 |
| Mn | <5.0 | < 10 |